Proceedings of the 2023 International Conference on Functional Materials and Civil Engineering
DOI: 10.54254/2755-2721/26/20230814

Evaluation, simulation, and empirical study of community microclimate comfort

Xiaoyu Chen

College of Architecture and Planning, Yunnan University, Kunming, Yunnan, 650224, China.

1191848333@qq.com

Abstract. Urban microclimates directly impact the comfort of living environments and human health. This study focuses on a community within a university in Guangzhou and constructs a corresponding index system from the perspectives of regional climate analysis and architectural layout. It summarizes the key spatial elements influencing thermal comfort in living environments. The results indicate: (1) Guangzhou is located in a typical hot-summer and warm-winter region, characterized by a humid climate; (2) Using a university community in Guangzhou, Guangdong, as the research subject, a comprehensive comparison is made between simulated and empirically measured comfort evaluations. A related factor analysis is conducted to identify the key factors affecting wind efficiency. Among these, variables such as daily average temperature at Panyu Station, average wind speed at Panyu Station, and average building height 50 meters from the sampling point are found to have correlations with both simulated and measured thermal comfort indicators; (3) The analysis reveals significant differences between simulated and actual comfort, primarily due to the influences of architectural layouts, spatial arrangements, and real environmental factors.

Keywords: Livable Community, Urban Climate Analysis, Wind Environment Simulation, Microclimate Comfort in Living Environments.

1. Introduction

Improving the urban microclimate has a direct impact on the residential environment. Sound urban planning can mitigate the urban heat island effect and enhance the comfort of living environments. Enhancing the urban microclimate and improving the environmental quality of neighborhoods are crucial issues in contemporary urban development.

Computational Fluid Dynamics (CFD) and other fluid mechanics simulation software have been widely applied in the optimization of microclimates. Related research has focused on various scales, including but not limited to regional [1, 2], urban [3, 4], block [5, 6], site [7], and indoor and outdoor thermal environments of group buildings [8-11]. However, current urban community planning and design often lack comprehensive analysis and assessment of target areas. Previous community planning and design in China have also often overlooked considerations for the urban microclimate. The regulations and requirements related to the urban microclimate in relevant norms and standards are expressed in relatively qualitative terms, lacking practical applicability.

In response to the shortcomings in previous research, this study focuses on a community within a university in Guangzhou. It summarizes the key spatial elements influencing thermal comfort in living environments from the perspectives of regional climate analysis and architectural layout. Based on the climatic conditions in Guangzhou during the autumn and winter seasons, meteorological indicators at both macro and micro scales in the target area are collected and empirically measured. The study analyzes the reasons for the differences between simulated and measured comfort levels.

2. Evaluation criteria and methods for thermal comfort in the wind-heat environment

2.1. Principles and steps of CFD simulation

The Phoenics software within Computational Fluid Dynamics (CFD) was utilized to simulate the wind environment in the research area. The process can be summarized as "preprocessing - simulation calculation - post-processing and visualization," as detailed in Figure 1.

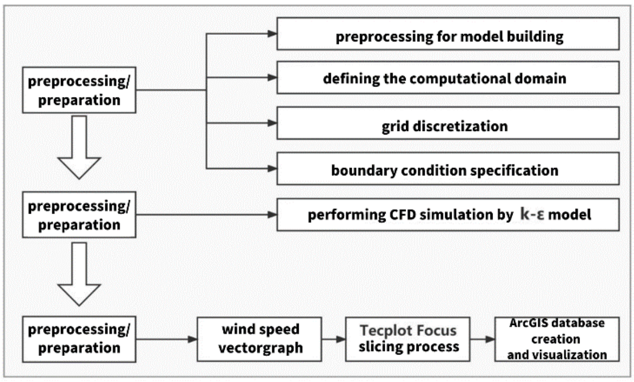

Figure 1. CFD simulation workflow.

2.2. Urban climate base analysis method

Because thermal balance indicators [12-15], such as PMV and PET, are more suitable for evaluating thermal comfort in steady-state environments and for individuals, this study refers to the "temperature-humidity index" and "wind effectiveness index" recommended in "Assessment of Climate Comfort in Human Living Environments." These two indicators are used to evaluate the thermal comfort of the target research area. When there are differences in the results of these two indicators, the wind effectiveness index is used during the winter half-year, and the temperature-humidity index is used during the summer half-year [16]. The formulas are as follows (1) to (3):

Temperature-Humidity Index:

$$I = 0.72(T + T_w) + 0.03J - 7.2\sqrt{u} + 40.6 \tag{1}$$

Comfort Variation:

$$\Delta I \begin{cases} I_t - I, & I \leq 60 \\ I - I_t, & I > 75 \end{cases} \tag{2}$$

Where:
I is the temperature-humidity index;
T is the average temperature during the evaluation period in degrees Celsius (°C);
RH is the average relative humidity during the evaluation period in percentage (%);
J is solar radiation intensity in W/m².

Wind Effectiveness Index:

$$I = -\left(10\sqrt{V} + 10.45 - V\right)(33 - T) + 8.55 \tag{3}$$

Where:
K is the wind effectiveness index;
T is the average temperature during the evaluation period in degrees Celsius (°C);

V is the average wind speed during the evaluation period in m/s;

S is the average daily sunshine duration during the evaluation period in hours per day (h/d).

Table 1. Classification of comfort level of living environment.

Level	Sensation	Temperature-Humidity Index	Wind Effectiveness Index	Perception by Healthy Individuals
1	Cold	<14.0	<-400	Feels very cold, uncomfortable
2	Cool	14.0~16.9	-400~-300	Somewhat cold, somewhat uncomfortable
3	Comfortable	17.0~25.4	-299~-100	Feels comfortable
4	Warm	25.5~27.5	-99~-10	Feels warm, somewhat uncomfortable
5	Hot	>27.5	>10	Feels hot, uncomfortable

2.3. Solar radiation intensity analysis model

A solar radiation intensity model established by previous researchers was used to analyze the spatial layout of the target research area. The formulas are as follows (4) to (6):

Total Solar Radiation:

$$G = G_{dir} + G_{dif} \tag{4}$$

Direct Solar Radiation:

$$\begin{cases} G_{dir} = S \cdot \beta^{m} - Dur \cdot SunGap \cdot \cos(AngIn) \\ m = \dfrac{\exp\left(-0.000118 \cdot Elev - 1.638 \cdot 10^{-9} \cdot Elev^{2}\right)}{cos\theta} \\ AngIn = \operatorname{acos}(cos\theta \cdot cosw + sin\theta \cdot sinw - \cos(\alpha - \gamma)) \end{cases} \tag{5}$$

Solar Radiation:**

$$\begin{cases} G_{dif} = R \cdot P_{dif} \cdot Dur \cdot SVF \cdot Weight \cdot \cos(AngIn) \\ R = \dfrac{S \cdot \sum \beta^{m}}{1 - P_{dif}} \end{cases} \tag{6}$$

Where:

G is the total solar radiation in J/m²;

G_{dir} is the direct solar radiation in J/m²;

G_{dif} is the diffuse solar radiation in J/m²;

S is the solar constant, 1367 W/m²;

β is the atmospheric transmittance for the shortest path;

m is the relative optical path length;

Dur is the duration of the solar chart sector in seconds;

$SunGap$ is the porosity of the solar chart sector;

$AngIn$ is the incident angle between the centroid of the solar chart sector and the normal axis of the surface in degrees (°);

$Elev$ is the elevation above sea level in meters (m);

θ is the zenith angle in degrees (°);

α is the azimuth angle in degrees (°);

w is the surface zenith angle in degrees (°);

y is the surface azimuth angle in degrees (°);
P_{dif} is the diffuse fraction, 0.2 for sunny days and 0.7 for overcast days;
SVF is the sky view factor;
$Weight$ is the proportion of this sky sector's area to the total sky area.

3. Results and analysis

3.1. Urban community wind-heat environment measurement

3.1.1. Climatic characteristics of the study area. Taking Guangzhou, Guangdong, China as an example, the region falls under a typical hot-summer and warm-winter climate zone. According to hourly observation data from Chinese meteorological stations provided by the National Meteorological Science Data Center (as shown in Figures 2 and 3), during the measurement period (from October 27, 2021, to November 25, 2021), Panyu Station recorded prevailing north winds (N) in Guangzhou, accounting for 20.56% of the total measurements. Following that, the most common wind directions were northeast winds (NNE, NE, ENE) with percentages of 17.88%, 13.25%, and 9.19%, respectively.

It can be concluded that during the measurement period in Guangzhou, the prevailing monsoon winds were predominantly from the north, followed by northwest winds and northeast winds. In the subsequent CFD simulation study, the analysis and simulation of the prevailing wind directions will be conducted based on wind frequencies, serving as the basis for simulating comfort. Additionally, collected climate base data will be correlated with building construction indicators, measurements, and the wind effectiveness index from simulations to explore the relationships between various indicators.

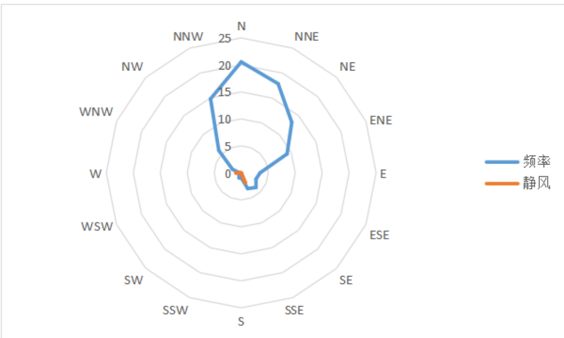

Figure 2. Wind direction frequency diagram of Panyu station in winter.

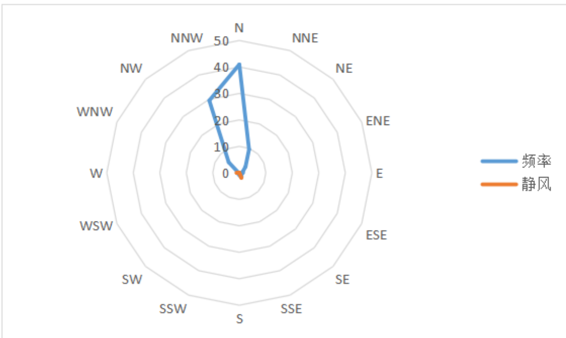

Figure 3. Wind direction frequency diagram of Guangzhou station in winter.

3.1.2. Measurement locations and time. The subject of this measurement is a university community in Guangzhou, Guangdong. According to detailed planning for construction purposes, the university's planned land area is approximately 451,876 square meters, with a building area of 459,773 square meters, and the overall layout is oriented from north to south.

During the measurements, 16 measurement points were placed around and within the building complex based on the building layout, spatial morphology, and other characteristics of the university campus. These points were established with consideration for differences in community volumetric ratio and building density, aiming to record wind-heat environmental characteristics in different spatial forms. The campus satellite image and measurement point layout are shown in Figure 4.

The testing period for this study was from 3:00 PM on October 19, 2021, to 3:00 PM on November 25, 2021. The measurement points were fixed on tripods and located approximately 1.5 meters above the ground. The measurement instruments used in the actual tests conformed to relevant national measurement regulations regarding their range and accuracy.

DOI: 10.54254/2755-2721/26/20230814

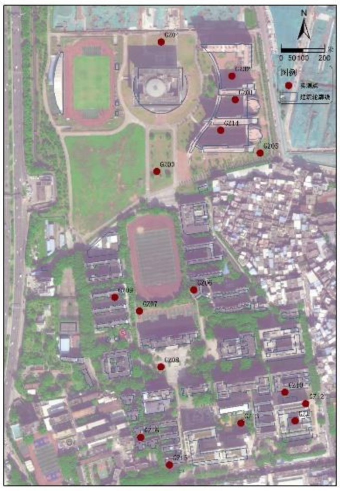

Figure 4. The measuring points of the test site

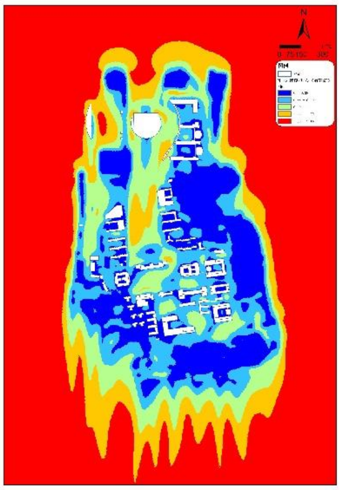

Figure 5. CFD wind environment simulation diagram (the inlet wind direction is N wind direction, with inlet wind speed at 2 m/s)

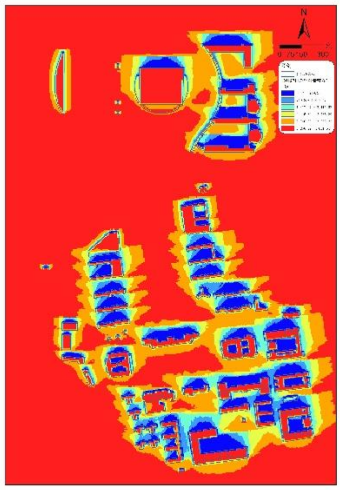

Figure 6. Simulation diagram of daily average radiation of headquarters campus(2022-10-27)

*3.1.3. Relative comfort simulation in the university community***.* Taking the north wind direction as an example, Figure 5 shows the CFD simulation based on the prevailing north winds during the measurement period in Guangzhou. The results closely match the wind speed distribution patterns during times when the wind blows through the community layout.

Using the solar radiation tools in ArcGIS, a solar radiation analysis was conducted on the target campus to determine the daily average radiation total for the study area, which is the sum of direct and diffuse radiation in WH/m² (as seen in Figure 6).

During the measurement period, Guangzhou was in the autumn-winter season. According to national standards, the study and analysis of thermal comfort in the measurement and simulation areas will be based on the "wind effectiveness index" indicator (as in equation 3 above) in the residential area national standard.

As shown in Table 2, the numerical values in the comfort difference section represent the day-by-day difference between measured comfort and simulated comfort. The closer these values are to zero (positive or negative), the closer the agreement between simulation and measurement results. Among these, the total number of effective measured days was 102 days, with 61 days having the same comfort results in both measurement and simulation, resulting in a simulation accuracy of 59.80%.

Table 2. Statistical table of comfort description differences between measurement and simulation.

Collection Point	Measured Days	Comparison of Measured and Simulated Comfort						
		Very Cold	Cold	Comfortable	Warm	Hot	Simulation Accuracy	Same Days
3 (Baseline Point)	25	0	0	8	-1	-7	68.00%	17
1	6	-3	-1	3	0	0	66.67%	4
2	7	0	1	1	-2	0	71.43%	5
4	5	0	0	3	-3	0	40.00%	2
5	3	0	0 (Same)	0 (Same)	0	0	100.00%	3
6	5	0	0	0(Same)	0	0	100.00%	5

Table 2. (continued).

7	3	0	0	0	0 (Same)	0	100.00%	3
8	3	0	0	0	-1	1	33.33%	1
9	7	0	0	0	3	-3	57.14%	4
10	6	0	0	0 (Same)	0 (Same)	0	100.00%	6
11	7	0	0	2	-2	0	71.43%	5
12	8	0	0	3	0	-2	37.50%	3
13	3	0	1	0	-1	0	66.67%	2
14	5	0	0	-1	1	0	20.00%	1
15	6	0	0	5	-5	0	0.00%	0
16	3	0	0	2	-2	0	0.00%	0
Total Accuracy							59.80%	

3.2. Impact of climatic environmental factors and construction control indicators on thermal comfort in the human living environment

3.2.1. Construction control indicators and the thermal comfort indicator system. In this study, the indicators affecting thermal comfort in the human living environment were determined using qualitative and quantitative research analysis methods. In the qualitative analysis process, these indicators can be categorized into two main groups: construction control indicators and climatic environmental indicators, with specific indicators listed in Table 3 below.

Table 3. Indicator system and classification for comfort evaluation.

Indicator Type	Scale	Number of Indicators	Indicator Names
Construction Control Indicators	50/100/150 meters (Circular Indicators) 50/100/150 meters (Measured Point Wind Frequency Sector Indicators) 50/100/150 meters (Panyu Station Wind Frequency Sector Indicators)	75	Paved Area, Paved Area Ratio, Building Base Area, Building Area, Building Density, Plot Ratio, Green Area, Green Area Ratio, Average Building Height, Distance to Nearest Building, Number of Trees
Climatic Environmental Indicators	Panyu Station Climatic Environmental Measured Indicators	4	Panyu Station Maximum Wind Frequency Wind Direction, Panyu Station Average Wind Speed (m/s at 10m), Panyu Station Calculated Wind Speed (m/s at 1.5 m), Measured Wind Speed Ratio
	Microscale Climatic Environmental Measured Indicators	8	Daily Average Humidity %, Daily Maximum Humidity %, Daily Minimum Humidity %, Daily Maximum Wind Speed (m/s), Daily Minimum Wind Speed (m/s), Daily Total Radiation J/m^2, Daily Average Radiation Intensity w/m^2, Daily Maximum Radiation Intensity w/m^2

DOI: 10.54254/2755-2721/26/20230814

Table 3. (continued).

Climatic Environ-mental Indicators	Microscale Climatic Environmental Simulation Indicators	9	Simulated Total Radiation J/m^2, Simulated Total Direct Radiation J/m^2, Simulated Total Scattered Radiation J/m^2, Simulated Direct Radiation Duration (h), Simulated Total Radiation Intensity w/m^2, Simulated Direct Radiation Intensity w/m^2, Simulated Wind Speed with Buildings (m/s at 1.5 m), Simulated Wind Speed without Buildings (m/s at 1.5 m), Simulated Wind Speed Ratio, Simulated Wind Speed (m/s)
Total	——	96	——

After the construction of the indicator system, the measured wind effectiveness index was used as the dependent variable, and Panyu Station climatic environmental indicators and microscale climatic environmental measured and simulated indicators were used as independent variables. This further refined the impact indicators for the dependent variable. Simultaneously, a comprehensive analysis of measured data within 50/100/150 meters for construction control indicators was performed to determine their impact on actual wind effectiveness index and derive research conclusions.

3.2.2. Correlation analysis of climatic environmental factors and construction control indicators on thermal comfort in the human living environment. As thermal comfort in the human living environment is influenced by both construction control indicators and climatic environmental factors, both aspects were included in the correlation analysis of thermal comfort to explore key indicator factors affecting thermal comfort in both simulated and measured environments.

Results of the correlation analysis are as follows:

(1) There are distinct patterns among the key influencing factors of the wind effectiveness index. Among meteorological environmental indicators, the daily average temperature at Panyu Station consistently exhibits correlation coefficients greater than 0.7, indicating a strong correlation with wind effectiveness index values. Correlation coefficients for factors related to daily maximum radiation intensity are consistently less than 0.2, suggesting a weak correlation. Within the construction control indicators, the average building height at a distance of 50 meters from the sampling point consistently shows negative correlation coefficients, with values near 0.3, indicating a significant correlation. This implies that within a 50-meter range, an increase in building height leads to a corresponding decrease in wind effectiveness index values.

(2) In the analysis of the actual environment (refer to Tables 4-5), climatic environmental factors play a decisive role in wind effectiveness index values. Factors such as the daily average temperature at Panyu Station and the maximum humidity at individual measured points exhibit significant correlations with the wind effectiveness index. Hence, it can be inferred that macro-regional climate base indicators, particularly temperature during the winter half-year, have a decisive impact on thermal comfort in the human living environment.

DOI: 10.54254/2755-2721/26/20230814

Table 4. Regression model for measured comfort (1) on climate and environmental factors and construction control indicators.

Model Fit Statistics	R	R-squared (R^2)	Adjusted R-squared	Standard Error of Estimate	
	0.929	0.863	0.853	46.42072 28642297 30	
Model Regression Coefficients and Significance Tests	**Unstandardized Coefficients Standardized Coefficients**		**Standardized Coefficients**	**t**	**Sig.**
	B	**Stan-dard Error**			
(Constant)	-560.210	38.438		-14.574	0.000
Daily Average Temperature at Panyu Station	21.598	1.649	0.831	13.098	0.000
Average Building Height (50 meters)	-1.724	0.337	-0.231	-5.113	0.000
Maximum Daily Humidity (%)	-2.459	0.359	-0.453	-6.845	0.000
Measured Wind Speed Ratio	-112.774	24.200	-0.198	-4.660	0.000
Daily Average Relative Humidity at Panyu Station	2.052	0.426	0.358	4.813	0.000
Calculated Wind Speed at Panyu Station (m/s)	19.193	8.606	0.110	2.230	0.028
Maximum Daily Radiation Intensity (w/m^2)	0.027	0.014	0.093	1.900	0.061
Average Daily Radiation Intensity (w/m^2)	-0.009	0.003	-0.136	-3.269	0.002
Number of Trees within 100 meters	0.123	0.052	0.096	2.382	0.019
Total Daily Radiation (J/m^2)	1.543E-6	0.000	0.103	2.230	0.028

(1) Dependent Variable: Measured Wind Efficiency Index at Observation Points; Independent Variables: Climate and Environmental Measurement Indicators at Panyu Station/Microenvironment and Construction Control Indicators.

DOI: 10.54254/2755-2721/26/20230814

Table 5. Regression model of measured comfort (2) on climate and environmental factors and construction control indicators.

Model Fit Statistics	R	R-squared (R^2)	Adjusted R-squared	Standard Error of Estimate	
	0.940	0.883	0.870	29.326999856564385	
Model Regression Coefficients and Significance Tests	Unstandardized Coefficients Standardized Coefficients		Standardized Coefficients	t	Sig.
	B	Standard Error			
(Constant)	-1415.991	429.046		-3.300	0.001
Daily Average Temperature at Panyu Station	21.675	1.370	0.834	15.825	0.000
Average Building Height (50 meters)	-1.932	0.365	-0.259	-5.288	0.000
Maximum Daily Humidity (%)	-2.307	0.330	-0.425	-6.999	0.000
Measured Wind Speed Ratio	-138.812	24.394	-0.244	-5.690	0.000
Daily Average Relative Humidity at Panyu Station	2.053	0.403	0.358	5.095	0.000
Simulated Wind Speed (m/s)	70.217	22.445	0.147	3.128	0.002
Simulated Direct Radiation Time (h)	-2.190	0.819	-0.104	-2.674	0.009
Maximum Daily Radiation Intensity (W/ m^2)	0.038	0.012	0.131	3.102	0.003
Average Daily Radiation Intensity (W/ m^2)	-.007	0.003	-0.103	-2.690	0.009
Number of Trees within 100 meters	0.244	0.110	0.084	2.219	0.029
Simulated Wind Speed without Buildings (m/s)	459.667	223.188	0.076	2.060	0.042

(2) Dependent Variable: Measured Wind Efficiency Index at Observation Points; Independent Variables: Climate and Environmental Measurements and Simulations at Panyu Station/Microenvironment, and Construction Control Indicators.

3.2.3. Correlation analysis of construction control indicators on human thermal comfort. In this section, an analysis of the correlation between construction control indicators and human thermal comfort is conducted. Specifically, this analysis involves extracting indicator values for the 50, 100, and 150-meter radial areas based on the measured highest daily wind frequencies at Panyu Station. The aim is to further investigate the correlation between construction control indicators and human thermal comfort. After regression analysis, it is found that only the indicator related to the 150-meter radial area of the highest daily wind frequency at Panyu Station can to some extent explain a portion of the model.

Table 6. Regression model of measured comfort (3) on climate and environmental factors and construction control indicators.

Model Fit Statistics	R	R-Square	Adjusted R-Square	Standard Error	
	0.462	0.214	0.200	79.11860	
Model Regression Coefficients and Significance Tests	Unstandardized Coefficients		Standardized Coefficients	t	Sig.
	B	Standard Error			
(Constant)	-150.540	19.150		-7.861	0.000
150-Meter Sector Building Area at PY Station	-0.004	0.001	-0.263	-2.982	0.004
150-Meter Sector Green Area at PY Station	0.025	0.009	0.257	2.920	0.004

(3) Dependent Variable: Measured Wind Efficiency Index at Observation Points; Independent Variables: Construction Control Indicators based on the 150-Meter Sector Range Wind Data at Panyu Station.

4. Conclusion

This paper, based on the evaluation methodology and process of climate analysis, has studied the concept and evaluation methods of human thermal comfort. It has analyzed the influencing factors of the wind-thermal environment and conducted empirical research supported by the detailed planning of a university community in Guangzhou.

(1) Guangzhou is located in a typical hot summer and warm winter region, characterized by a relatively humid climate. Additionally, the region experiences prevailing north winds during the winter season. Among these, measurements at Panyu Station indicate that the predominant wind direction during the observed period in Guangzhou is the north wind (N), accounting for 20.56% of the total measurements.

(2) Using a university community in Guangzhou as the research subject, a comparative analysis was performed based on the comprehensive assessment results of measured comfort. Concurrently, a analysis of relevant factors was conducted to identify the key influencing factors of the wind effectiveness index. Notably, factors such as the daily average temperature at Panyu Station, the average wind speed at Panyu Station, and the average building height at a distance of 50 meters from the sampling point are all correlated with the measured thermal comfort indicators.

(3) Climate environmental factors play a decisive role in the values of the wind effectiveness index. Particularly, macroscopic regional climate baseline indicators, especially temperature, will have a decisive impact on the comfort of the living environment during the winter half of the year.

References

[1] Liang, H. Y. (2018). Research on the Impact Factors and Evaluation Model of Urban Controlled Detailed Planning Thermal Environment [Doctoral dissertation, South China University of Technology].

DOI: 10.54254/2755-2721/26/20230814

[2] Wang, Z., & Xia, R. (2008). Research on Block-Level Canyon Climate Adaptive Design Strategies in Hot Summer and Cold Winter Regions [Doctoral dissertation, Huazhong University of Science and Technology].
[3] Wang, X. Y. (2007). Quantitative Analysis Techniques for Urban Planning Atmospheric Environment Effects [Book]. Meteorological Press.
[4] Bai, C. (2009). Urban Climate Design [Book]. China Architecture & Building Press.
[5] Qin, W. C. (2015). Numerical Simulation of Urban Microclimate at the Block Scale [Doctoral dissertation, Southwest University].
[6] Wu, S. L., & Sun, Y. M. (2015). Analysis of the Impact of Urban Design Elements on the Urban Heat Island Effect: A Case Study of Guangzhou. Journal of Architecture, 10, 79-82.
[7] Wang, P., Meng, Q. L., et al. (2013). Preliminary Exploration of CBD Green Buffer Zone Application. Urban Planning, 37(5), 74-77.
[8] Meng, Q. L., Zhang, L., Zhao, L. H., et al. (2012). Introduction to the Chinese Industry Standard "Urban Residential Area Thermal Environment Design Standard" [Conference Paper]. National Building Physics Academic Conference. China Architecture Society.
[9] Wang, C. Y. (2008). Analysis and Simulation of Urban Thermal Environment Based on Remote Sensing and CFD Technology [Doctoral dissertation, Lanzhou University].
[10] Zhu, X. W. (2012). Simulation Study on Urban Microclimate in Small Neighborhoods in Hot Summer and Warm Winter Areas [Doctoral dissertation, Harbin Institute of Technology].
[11] Nakamura, Y., & Hirano, W. (1986). Study on Surface Temperature Heat Flux Analysis of Two-Dimensional Rectangular Block Street Space. Journal of Architectural Planning, No. 367.
[12] Wang, F., Wang, S. G., & Zhang, T. F. (2014). CFD Indoor Environmental Simulation Based on Outdoor Meteorological Information. Building Thermal Energy, Ventilation and Air Conditioning, 33(02), 23-27.
[13] Zheng, J., & Wang, G. G. (2019). Application of Microclimate Environment Simulation and Scheme Optimization in Traditional Block Renewal: A Case Study of Zhaoping Baogongfu Block. Planner, 35(15), 79-86.
[14] Wang, F., Wang, S. G., & Zhang, T. F. (2014). CFD Indoor Environmental Simulation Based on Outdoor Meteorological Information. Building Thermal Energy, Ventilation and Air Conditioning, 33(02), 23-27.
[15] Wang, J. (2012). Research on Building Layout Strategies in Shenzhen's Riverside District Based on Wind Environment [Doctoral dissertation, Harbin Institute of Technology].
[16] JGJ 286-2013. (2014). Urban Residential Area Thermal Environment Design Standard [Book]. China Architecture & Building Industrial Press.